Mechanical properties and anisotropy of AZ31 alloy sheet processed by flat extrusion container

Qingshan Yang
Material Science Department, College of Materials Science and Engineering, Chongqing University, Chongqing 400044, China; and Laboratory for Rolling of Mg Alloy, National Engineering Research Center for Magnesium Alloys, Chongqing University, Chongqing 400044, China

Bin Jiang[a)]
Material Science Department, College of Materials Science and Engineering, Chongqing University, Chongqing 400044, China; Laboratory for Rolling of Mg Alloy, National Engineering Research Center for Magnesium Alloys, Chongqing University, Chongqing 400044, China; and Light Alloy Department, Chongqing Academy of Science and Technology, Chongqing 401123, China

Jiahong Dai and Ruihong Li
Material Science Department, College of Materials Science and Engineering, Chongqing University, Chongqing 400044, China

Fusheng Pan
Laboratory for Rolling of Mg Alloy, National Engineering Research Center for Magnesium Alloys, Chongqing University, Chongqing 400044, China; and Light Alloy Department, Chongqing Academy of Science and Technology, Chongqing 401123, China

(Received 17 October 2012; accepted 28 February 2013)

The microstructure evolution and mechanical responses are investigated in uniaxial tensile test performed on AZ31 magnesium alloy sheets processed by the flat extrusion container. A novel emphasis based on the texture was used to estimate the relative magnitude of hardening effects related to the deformation twinning. The anisotropic behavior of the sheets is sensitive to the orientation of the crystals with respect to the loading direction. This is ascribed to the effect of the initial texture and the activation of their relative critical resolved shear stresses on slip and twinning. The increased accumulated hardening increases the twin nucleation stress. The deformation twinning significantly induces an asymmetry in the yield behavior. Moreover, it remarkably prolongs the slope of the stage II in the working hardening curve. An accepted notion is proposed that the preferential activity of deformation twinning exerts a significant effect on mechanical anisotropy during tension.

I. INTRODUCTION

The applications of magnesium alloys are being increasingly evaluated for aerospace and automotive components due to the combination exhibited by them of high specific strength, low density and excellent machinability.[1–4] Compared with their casting counterparts, wrought magnesium alloys have much better mechanical properties.[5] However, most deformed magnesium alloys usually give rise to a strong texture during the primary processing such as extrusion and rolling, which is related to their limited number of active deformation systems in hexagonal close-packed (hcp) crystal structure. This leads to a high directional anisotropy of mechanical properties.[6,7] In general, basal $<a>$ slip systems can easily activate in magnesium (Mg) alloys at room temperature, while the prismatic $<a>$ and the pyramidal $<a+c>$ slip systems can operate only if a higher driving force is given or deformed at elevated temperature because of their high critical resolved shear stresses (CRSSs).[8] This can further limit the expanded application of magnesium alloys. It can be seen that the texture has an intensive effect on their deformation and fracture characteristic, which would enhance or deteriorate the complicity of the mechanical behavior.[9–12]

The hot flat extrusion is a squeezing process that compresses an initial billet in a container to produce long parts with constant cross-sections at elevated temperatures.[13,14] The process has considerable geometric similarity with sectional material and the metals, so that the metals flow more evenly, which enables them to be supplied with good dimensional accuracy, as shown in Fig. 1. It becomes one of the most economic and simple manufacturing processes. Although a large amount of investigations have dealt with the mechanical behavior of extruded magnesium alloys, much less attention has been paid to establish a qualitative or quantitative correlation among deformation mechanisms, texture and mechanical anisotropy of the FEC-processed magnesium alloy sheets. In addition, the strain hardening behavior is closely related with cold workability.

[a)]Address all correspondence to this author.
e-mail: jiangbinrong@cqu.edu.cn
DOI: 10.1557/jmr.2013.51

 © Materials Research Society 2013

https://doi.org/10.1557/jmr.2013.51 Published online by Cambridge University Press

Thus, the comprehension of the strain hardening behavior of Mg alloy sheet is crucial for optimizing the parameters for deformation processing.[15]

In this work, the anisotropic effects on the strain hardening rate dependence are investigated of the as-received FEC-processed AZ31 magnesium alloy sheet with an addition of cerium. A substantial body of research has established that the addition of cerium to the AZ31 magnesium alloy resulted in efficient grain refining. The well-dispersed and thermally stable MgAlCeMn second phase particles protect grain growth and postpone cavitation to higher strain levels to enhance hot formability.[16–19] The AZ31 magnesium alloy sheets produced by FEC processing present a more complex case because the twinning also plays an important role during deformation. Twinning makes slip more or less favorable owing to the reorientation of crystal lattice so that it affects the strain hardening and softening behavior.[7] This work has assumed the aforementioned hypotheses for the mechanisms responsible for different morphologies of the tensile twins in the alloy.

II. EXPERIMENTAL

The as-received AZ31 magnesium alloy sheet was produced by FEC processing and the alloy compositions are given in Table I. The size of the sheets was 600 mm in length in the extrusion direction (ED), 500 mm in width in the transverse direction (TD) and 3 mm in thickness in the normal direction, (ND). Dog-bone tensile samples of 60 mm in gage length, 12.5 mm in width and 3 mm in thickness were machined from the sheets with various directions tilting 0, 30, 45, 60 and 90° to ED, respectively, as illustrated in Fig. 2. Tensile tests were performed at an initial strain rate of 10^{-3}/s using a universal testing machine (UTM. model No. CMT6305-300 KN, SUNS, Shenzhen, China) at room temperature.

The microstructures were examined by optical microscopy (OM). The (0002) pole figures of AZ31 magnesium alloy were determined using an x-ray diffractometer (XRD; Rigaku model No. D/Max 2500, Rigaku, Tokyo, Japan) with Cu K_α radiation, a voltage of 40 kV and a current of 100 mA. Fracture morphologies surfaces of tensile samples were observed in detail by scanning electron microscopy (SEM). The electron backscatter diffraction data was collected using a diffractometer (EBSD; HKL Channel 5 System equipped with FEI Nova 400 FEG-SEM, Cambridge, MA).

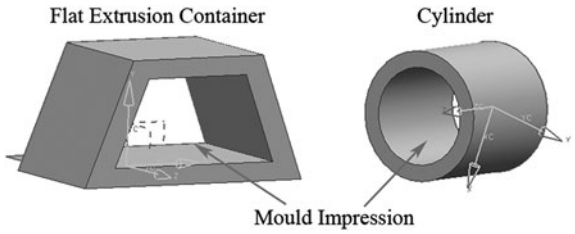


FIG. 1. Diagrammatic sketch of flat extrusion container and cylinder.

TABLE I. Chemical composition of the studied alloy (in wt%).

Al	Zn	Mn	Ce	Mg
3.32	0.94	0.3	0.71	Balance

III. RESULTS AND DISCUSSION

A. Microstructural characterization

As shown in Fig. 3(a), the microstructures of AZ31 magnesium alloy sheet are observed from the transverse section (ND-TD plane) and the longitudinal section (ND-ED plane), respectively. The magnesium alloys are characterized by inhomogeneous microstructure with few finer equiaxed dynamically recrystallized (DRX) grains of about 20 μm embedded in relatively large zones of elongated deformed grains of about 100 μm. Figure 3(b) illustrates (0002) pole figure of AZ31 magnesium alloy sheet. It principally remains a basal texture and with some *c*-axis orientation of basal planes rotated to TD.

B. The mechanical behavior of AZ31 magnesium alloy sheet

The true stress–strain curves measured on different directions in each group (at least three samples were tested in each group) were found to exhibit variance in Fig. 4. It confirms the strong anisotropy of stress–strain behavior

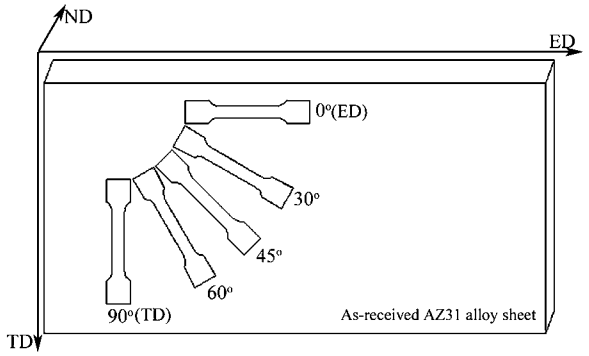


FIG. 2. Schematic diagram of specimen orientations for tensile tests.

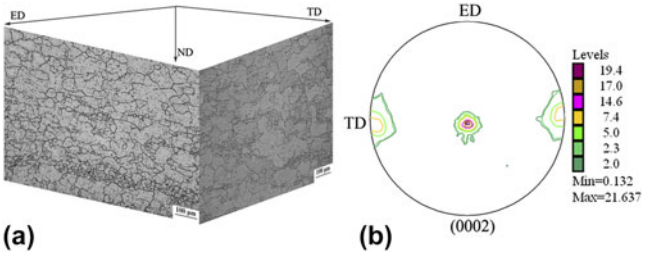


FIG. 3. (a) Different direction of OM micrographs in the AZ31 sheet and (b) measured (0002) pole figure of the corresponding alloy.

https://doi.org/10.1557/jmr.2013.51 Published online by Cambridge University Press

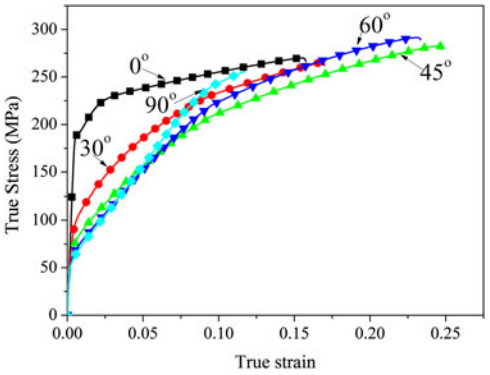


FIG. 4. True stress-strain curves during tensile tests in different directions.

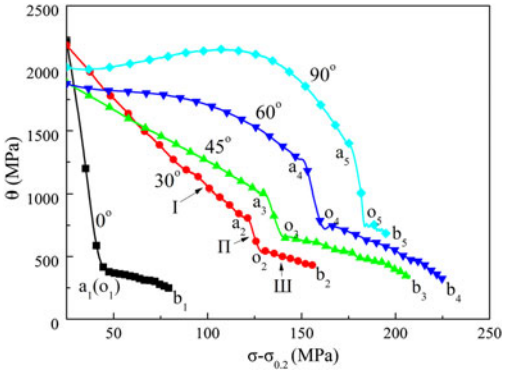


FIG. 5. Influence of the angle to extrusion direction on the WH behavior of the AZ31 magnesium alloy.

TABLE II. Results of the tensile tests carried out in the tensile directions of 0, 30, 45, 60 and 90°.

Angle to ED	YS (Mpa)	UTS (Mpa)	FE (%)	*n*-value
0°	188.6	268.1	15.5	0.10
30°	106.1	264.8	16.3	0.31
45°	73.7	280.6	23.8	0.38
60°	64.2	289.9	21.6	0.45
90°	58.8	258.2	12.9	0.52

exhibited by the AZ31 sheet with respect to the initial texture. To describe and compare conveniently, mechanical properties of the 0.2% proof yield stress (YS), the ultimate tensile strength (UTS), the failure elongation (FE) and the strain-hardening exponent value (*n*-value) for the sheets are listed in Table II. When increasing the angle to the extrusion direction, the yield stress sharply decreases from 188.6 to 58.8 Mpa and *n*-value increases from 0.10 to 0.52 simultaneously. The stress-strain curves show high yield stress and low strain hardening rate for the 0° sample, low yield stress and high strain hardening rate for the 90° sample. These differences are caused by the in-plane variations in the texture and the resulting variations in the basal slip activities and nonbasal $<a>$ type dislocations.[20]

The strain hardening anisotropy of the AZ31 magnesium alloy was also examined. It is well known that the macroscopic hardening rate can be expressed as $\theta = d\sigma/d\varepsilon$, where σ, $\sigma_{0.2}$ and ε are the macroscopic true stress, 0.2% proof yield stress and true plastic strain, respectively.[21,22] The work hardening rate θ versus net flow stress ($\sigma-\sigma_{0.2}$) curves of the extruded alloy is presented in Fig. 5. The $\sigma-\sigma_{0.2}$ shows the relation between the dislocation contribution and the flow stress. The anisotropy of strain hardening in all specimens is considerable in the stage III. It is seen that 0° specimen exhibits first a rapid strain hardening decrease after yielding due to a short elastoplastic transition, and then a relatively low reduction tendency of hardening associated with the stage III of strain hardening. The differential work hardening (WH) behavior can be attributed to the fact that differences in grain orientation can easily alter the resolved shear stress on basal planes and also favor the activation of nonbasal slip systems.[21] The curves (o_1b_1, o_2b_2, o_3b_3, o_4b_4, and o_5b_5 are shown in Fig. 5) are quite parallel at room temperature. This indicates that the dynamic recovery, associated with the slope during stage III of WH, is almost the same irrespective of the angle to extrusion direction. Additionally, it is interesting to note that the length of the curves (a_1o_1, a_2o_2, a_3o_3, a_4o_4, and a_5o_5) of stage II has an obvious increase with orientations tilting toward the ED. It may be related to the accumulation of geometrically necessary dislocations, but requires further study and reliable data to support. Taking into account that deformation twinning can produce an extra-hardening effect acting as obstacles to the dislocation slip, it is reasonable to have less hardening if twinning activity is limited.[23] The tensile twinning activity was studied using optical metallography and EBSD inverse pole figure maps in Fig. 6. It is expected that the formation of tensile twins are the source of the effects in samples with a marked basal texture. It can be noted that the twins have obviously increased with the angle of tilting increasing towards the extrusion direction of tensile samples. A significant proportion of boundaries associated with $\{10\bar{1}2\}$ extension twins are shown in Fig. 6(g). The twinning is generated during loading in the different tensile directions in response to the local stress states caused by the deformation of neighboring grains.[24] The activity of deformation modes in magnesium alloys are composed of basal slip along $<11\bar{2}0>$ ($<a>$) direction, nonbasal slip ($\{10\bar{1}0\}$-prismatic, $\{10\bar{1}1\}$-pyramidal) and twinning. The plastic deformation can be evaluated by the calculation of the CRSSs. It can be generally accepted that $CRSS_{basal} < CRSS_{twinning} < CRSS_{prismatic} < CRSS_{pyramidal}$ in Mg alloys.[25,26] The resolved shear stress on basal planes along the hcp crystal's *c*-axis increases with increasing the angle to extrusion direction because of the strong basal texture associated with some *c*-axis orientations rotating to TD, as

https://doi.org/10.1557/jmr.2013.51 Published online by Cambridge University Press

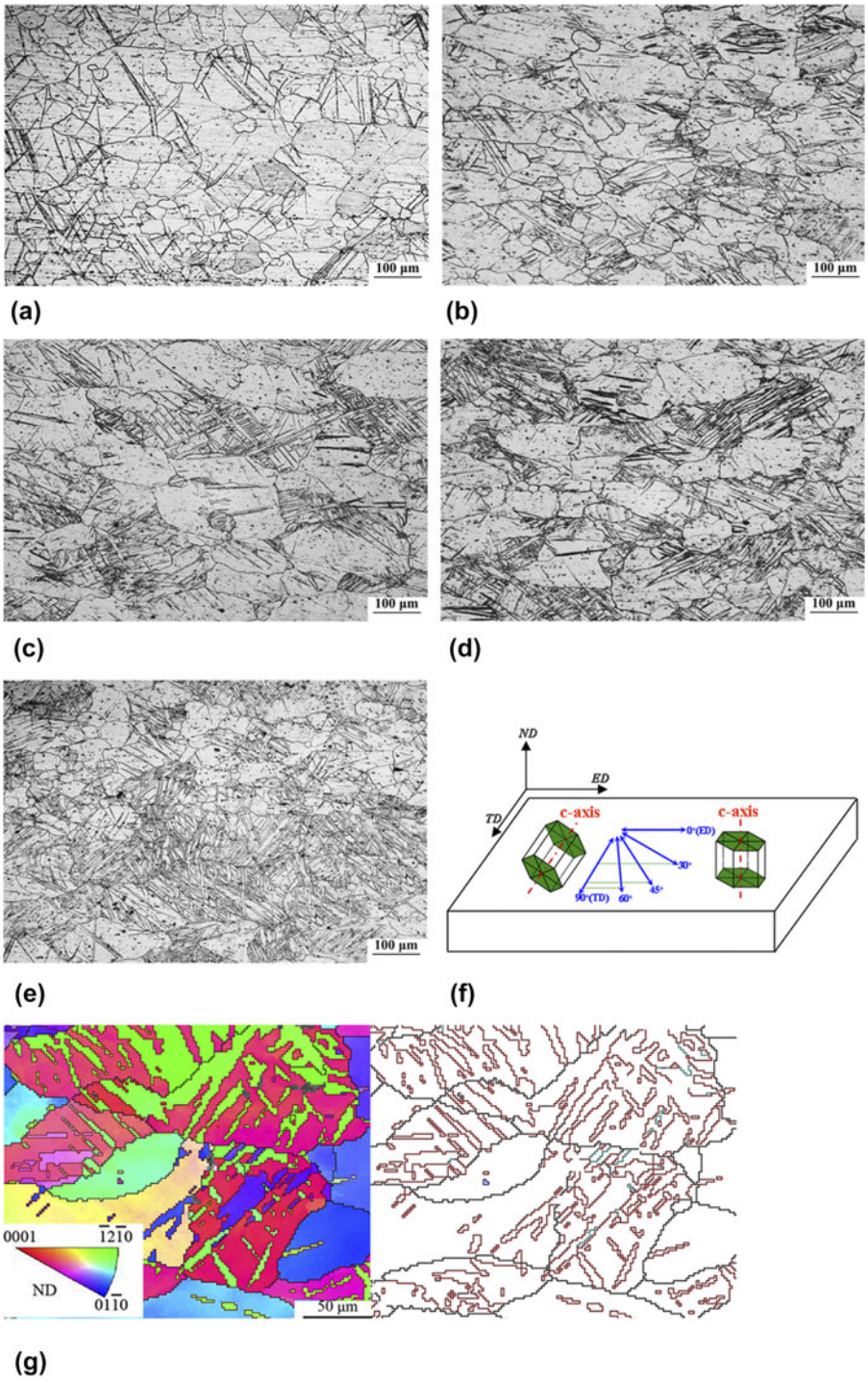


FIG. 6. Microstructures of tensile samples corresponding to a true strain of 0.08: (a) 0°; (b) 30°; (c) 45°; (d) 60°; (e) 90°. (f) Illustration of the orientation of tensile direction with respect to the *c*-axis. (g) EBSD inverse pole figure (IPF) maps of 90° sample.

shown in Fig. 6(f). It indicates that the basal slip dominates at the beginning of deformation. Afterward twinning is activated to accommodate the deformation as the stress reaches a sufficient enough high level.[15]

The texture hardening worked as the main contributor promoting extension twinning causing strain hardening in the tensile samples. Extension twins make grains rotate into hard orientations with the *c*-axis more or less parallel to the loading axis. The samples exhibited very different strain-hardening rates after the initiation of plastic strain, which resulted in a tension asymmetry in the offset yield values.[27,28] Additionally, the inclination of the *c*-axes may

https://doi.org/10.1557/jmr.2013.51 Published online by Cambridge University Press

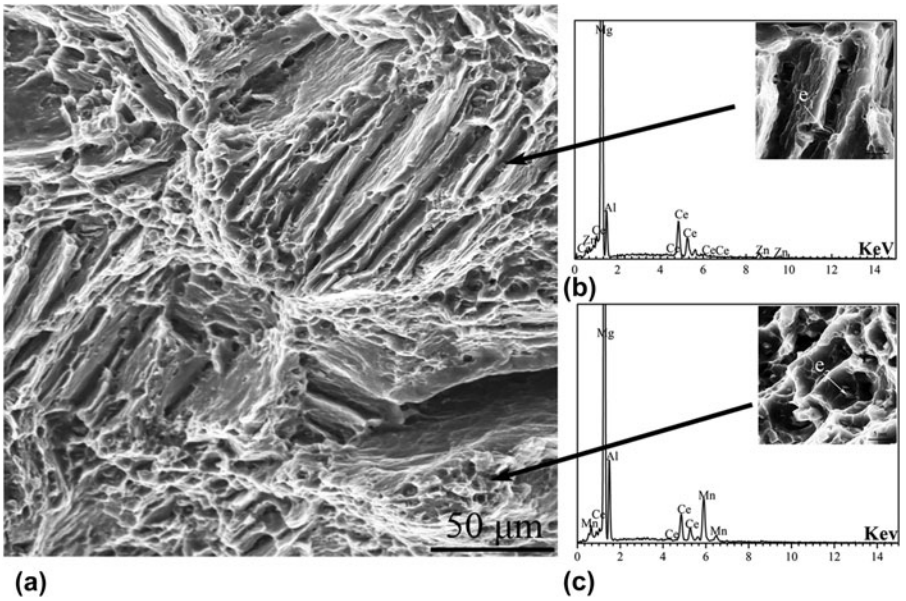


FIG. 7. Tensile fracture surface morphologies of 45° sample and energy-dispersive spectroscopy (EDS) analysis of the bright particles at points.

also increase the n-value due to the restricted dynamic recovery and activated $\{10\bar{1}2\}$extension twinning.[29] The differential work hardening rates in relation to the tilting angles towards the ED are treated as changes taking place in CRSSs arising out of deformation. If the production of deformation twins alters the stress field in the deformation systems, it will lead to the additional heterogeneity. The loss of coherency at the twin–matrix boundary can subsequently be raised by any such heterogeneity. The results suggest that the twinning effect of the yield behavior is more outstanding than one of the slip. Meanwhile, the mechanical behavior is controlled to a great extent by the crystal orientation related to deformation modes.[15] Several studies have been reported that twins can refine the grains and reduce the effective slip distance of dislocation, which would raise the strain-hardening rate at stage II as a result of the effect of deformation twinning boundaries.[30,31] The length of stage II is determined by the volume fraction of deformation twinning. The activation of deformation twinning may depend on the availability of a critical level of dislocation density due to initial dislocation generation and motion in the specimens.[23]

The different fracture modes of samples, after tension to failure, should be associated with the difference in their elongations. Two deformation mechanisms, such as twinning and slip that can make more plastic strain, can bring about the occurrence of necking and high elongation in their tensile fractures. For the 0° sample, the basal slip is easily activated, and the tensile failure displays obvious shearing feature, whereas for the 90° sample, twinning plays a dominant role in the deformation. Figure 7 depicts tensile fracture surface morphologies and energy-dispersive spectroscopy (EDS) results. Figures 7(b) and 7(c) are partial enlargements of Fig. 7(a). A large amount of plastic dimples and cracked particles, which are characterized by the ductile failure, can be observed on the fracture surface. EDS analysis shows that the chemical composition of the particles is consistent with MgAlCeMn second phases. In addition, the sheet consists of coarse grains with large number of second phases, which result in the accumulation of dislocation entanglement, as shown in Fig. 8(a). It also can be seen that a great deal of particles of second phases exist around the twins after tensile fracture in Fig. 8(b). Thus, the twinning is a predominant factor in the generalized deformation during tensile tests.

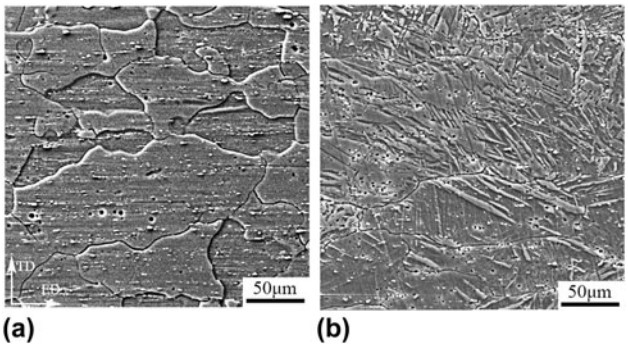


FIG. 8. SEM images for (a) as-received AZ31 sheet and (b) fractured tensile samples.

IV. CONCLUSIONS

The present work demonstrates that the interaction between the texture and deformation twins have a great influence on the mechanical anisotropy and the work hardening of as-received AZ31 magnesium alloy sheets

https://doi.org/10.1557/jmr.2013.51 Published online by Cambridge University Press

processed by flat extrusion container. The volume fraction of twins in 0, 30, 45, 60 and 90° samples have gradually increased due to the effect through different angles between *c*-axis and loading direction in the tensile tests. This significantly induces an asymmetry in the yield behavior. Meanwhile, it prolongs the slope of stage II in the working hardening curve. The important contribution to increasing the strain-hardening rate with the consequent texture strengthening makes grain orientations rotate into hard orientations as result of the deformation twinning. Twinning is deemed to be an acceptable deformation mechanism in coarse grain sizes during tensile tests and plays a crucial role in WH compared with texture effects.

ACKNOWLEDGMENTS

The authors are grateful to the financial supports from National Natural Science Foundation of China (Grant No. 51171212), Chongqing Science & Technology Commission (Grant Nos. 2010CSTC-HDLS, CSTC2010AA4048, CSTC2012JJJQ50001), China National Funds for Distinguished Young Scientists (Grant No. 50725413), The National Industrialization Technology and Development Program of China (Grant No. 2011BAE22B03-3) and Fundamental Research Funds for the Central Universities (Grant No. CDJXS12131106).

REFERENCES

1. I. Ulacia, N.V. Dudamell, F. Gálvez, S. Yi, M.T. Pérez-Prado, and I. Hurtado: Mechanical behavior and microstructural evolution of a Mg AZ31 sheet at dynamic strain rates. *Acta Mater.* **58**, 2988–2998 (2010).
2. S.R. Agnew and Ö. Duygulu: Plastic anisotropy and the role of non-basal slip in magnesium alloy AZ31B. *Int. J. Plasticity* **21**, 1161–1193 (2005).
3. S.M. Masoudpanah and R. Mahmudi: The microstructure, tensile, and shear deformation behavior of an AZ31 magnesium alloy after extrusion and equal channel angular pressing. *Mater. Des.* **31**, 3512–3517 (2010).
4. G. Wan, B.L. Wu, Y.D. Zhang, G.Y. Sha, and C. Esling: Anisotropy of dynamic behavior of extruded AZ31 magnesium alloy. *Mater. Sci. Eng., A* **527**, 2915–2924 (2010).
5. X. Lou, M. Li, R. Boger, S. Agnew, and R. Wagoner: Hardening evolution of AZ31B Mg sheet. *Int. J. Plasticity* **23**, 44–86 (2007).
6. S. Seipp, M.F.X. Wagner, K. Hockauf, I. Schneider, L.W. Meyer, and M. Hockauf: Microstructure, crystallographic texture and mechanical properties of the magnesium alloy AZ31B after different routes of thermo-mechanical processing. *Int. J. Plasticity* **35**, 155–166 (2012).
7. L. Wu, A. Jain, D.W. Brown, G.M. Stoica, S.R. Agnew, B. Clausen, D.E. Fielden, P.K. Liaw: Twinning–detwinning behavior during the strain-controlled low-cycle fatigue testing of a wrought magnesium alloy, ZK60A. *Acta Mater.* **56**, 688–695 (2008).
8. D.K. Xu, L. Liu, Y.B. Xu, and E.H. Han: Effect of microstructure and texture on the mechanical properties of the as-extruded Mg–Zn–Y–Zr alloys. *Mater. Sci. Eng., A* **443**, 248–256 (2007).
9. T. Al-Samman, X. Li, and S.G. Chowdhury: Orientation dependent slip and twinning during compression and tension of strongly textured magnesium AZ31 alloy. *Mater. Sci. Eng., A* **527**, 3450–3463 (2010).
10. C. Bruni, A. Forcellese, F. Gabrielli, and M. Simoncini: Effect of temperature, strain rate and fibre orientation on the plastic flow behaviour and formability of AZ31 magnesium alloy. *J. Mater. Process. Technol.* **210**, 1354–1363 (2010).
11. H.L. Kim, W.K. Bang, and Y.W. Chang: Deformation behavior of as-rolled and strip-cast AZ31 magnesium alloy sheets. *Mater. Sci. Eng., A* **528**, 5356–5365 (2011).
12. F. Lv, F. Yang, Q.Q. Duan, Y.S. Yang, S.D. Wu, S.X. Li, Z.F. Zhang: Fatigue properties of rolled magnesium alloy (AZ31) sheet: Influence of specimen orientation. *Int. J. Fatigue* **33**, 672–682 (2011).
13. G-A. Lee, D-Y. Kwak, S-Y. Kim, and Y-T. Im: Analysis and design of at-die hot extrusion process 1. Three-dimensional finite element analysis. *Int. J. Mech. Sci.* **44**, 915–934 (2002).
14. G-A. Lee and Y-T. Im: Analysis and die design of at-die hot extrusion process 2. Numerical design of bearing lengths. *Int. J. Mech. Sci.* **44**, 935–946 (2002).
15. B. Wang, R. Xin, G. Huang, and Q. Liu: Effect of crystal orientation on the mechanical properties and strain hardening behavior of magnesium alloy AZ31 during uniaxial compression. *Mater. Sci. Eng., A* **534**, 588–593 (2012).
16. L. Shang, S. Yue, R. Verma, P. Krajewski, C. Galvani, and E. Essadiqi: Effect of microalloying (Ca, Sr, and Ce) on elevated temperature tensile behavior of AZ31 magnesium sheet alloy. *Mater. Sci. Eng., A* **528**, 3761–3770 (2011).
17. X. Li, T. Al-Samman, and G. Gottstein: Mechanical properties and anisotropy of ME20 magnesium sheet produced by unidirectional and cross rolling. *Mater. Des.* **32**, 4385–4393 (2011).
18. L. Shang, I.H. Jung, S. Yue, R. Verma, and E. Essadiqi: An investigation of formation of second phases in microalloyed, AZ31 Mg alloys with Ca, Sr and Ce. *J. Alloys Compd.* **492**, 173–183 (2010).
19. W. Li, H. Zhou, P. Lin, and S. Zhao: Microstructure and rolling capability of modified AZ31–Ce–Gd alloys. *Mater. Charact.* **60**, 1298–1304 (2009).
20. A. Jain, O. Duygulu, D.W. Brown, C.N. Tomé, and S.R. Agnew: Grain size effects on the tensile properties and deformation mechanisms of a magnesium alloy, AZ31B, sheet. *Mater. Sci. Eng., A* **486**, 545–555 (2008).
21. J.A. del Valle, F. Carreño, and O.A. Ruano: Influence of texture and grain size on work hardening and ductility in magnesium-based alloys processed by ECAP and rolling. *Acta Mater.* **54**, 4247–4259 (2006).
22. R. Xin, B. Song, K. Zeng, G. Huang, and Q. Liu: Effect of aging precipitation on mechanical anisotropy of an extruded Mg–Y–Nd alloy. *Mater. Des.* **34**, 384–388 (2012).
23. M. Knezevic, A. Levinson, R. Harris, R.K. Mishra, R.D. Doherty, and S.R. Kalidindi: Deformation twinning in AZ31: Influence on strain hardening and texture evolution. *Acta Mater.* **58**, 6230–6242 (2010).
24. M.D. Nave and M.R. Barnett: Microstructures and textures of pure magnesium deformed in plane-strain compression. *Scr. Mater.* **51**, 881–885 (2004).
25. A. Styczynski, C. Hartig, J. Bohlen, and D. Letzig: Cold rolling textures in AZ31 wrought magnesium alloy. *Scr. Mater.* **50**, 943–947 (2004).
26. P. Liu, Y-C. Xin, and Q. Liu: Plastic anisotropy and fracture behavior of AZ31 magnesium alloy. *Trans. Nonferrous Met. Soc. China* **21**, 880–884 (2011).
27. S. Yi, J. Bohlen, F. Heinemann, and D. Letzig: Mechanical anisotropy and deep drawing behaviour of AZ31 and ZE10 magnesium alloy sheets. *Acta Mater.* **58**, 592–605 (2010).
28. S.B. Yi, C.H.J. Davies, H.G. Brokmeier, R.E. Bolmaro, K.U. Kainer, and J. Homeyer: Deformation and texture evolution in AZ31 magnesium alloy during uniaxial loading. *Acta Mater.* **54**, 549–562 (2006).

https://doi.org/10.1557/jmr.2013.51 Published online by Cambridge University Press

29. X. Huang, K. Suzuki, and N. Saito: Textures and stretch formability of Mg–6Al–1Zn magnesium alloy sheets rolled at high temperatures up to 793K. *Scr. Mater.* **60**, 651–654 (2009).
30. L. Jiang, J.J. Jonas, R.K. Mishra, A.A. Luo, A.K. Sachdev, and S. Godet: Twinning and texture development in two Mg alloys subjected to loading along three different strain paths. *Acta Mater.* **55**, 3899–3910 (2007).
31. M.R. Barnett, Z. Keshavarz, A.G. Beer, and D. Atwell: Influence of grain size on the compressive deformation of wrought Mg–3Al–1Zn. *Acta Mater.* **52**, 5093–5103 (2004).

https://doi.org/10.1557/jmr.2013.51 Published online by Cambridge University Press